Kinetic and Structural EPR Studies of Radical Polymerization. Monomer, Dimer, Trimer and Mid-chain Radicals formed *via* the Initiation of Polymerization of Acrylic Acid and Related Compounds with Electrophilic Radicals ($^{\bullet}OH$, $SO_4^{-\bullet}$ and $Cl_2^{-\bullet}$)

Bruce C. Gilbert,[a] John R. Lindsay Smith,[a] Elizabeth C. Milne,[a] Adrian C. Whitwood[a] and Philip Taylor[b]

[a] *Department of Chemistry, University of York, Heslington, York, UK YO1 5DD*
[b] *Research Department, ICI Paints plc, Wexham Road, Slough, UK*

A continuous-flow system has been used in conjunction with EPR spectroscopy to study the initial stages of polymerization of acrylic acid and methacrylic acid in aqueous solution at pH 2 and 9, brought about with inorganic radicals (*e.g.* $^{\bullet}OH$) formed from metal–peroxide redox couples. Structural characteristics of monomer adduct-radicals, as well as corresponding dimers and trimers, are reported, together with evidence for rapid intramolecular hydrogen-abstraction of the appropriate tetramer to give a mid-chain radical. Computer-based simulation of steady-state concentrations leads to estimates of rate constants for initiation, propagation and termination reactions under these conditions.

EPR spectroscopy has been used in conjunction with continuous-flow experiments to demonstrate the feasibility of detecting 'monomer', 'dimer' and polymer radicals during the early stages of free-radical-initiated polymerization of some water-soluble alkenes (see *e.g.* refs. 1–3). In extending this study to the investigation of the polymerization of acrylic acid and related compounds with initiators such as $^{\bullet}OH$ and $SO_4^{-\bullet}$ (at both low and high pH) we had two particular aims; the first was to explore the ways in which EPR spectroscopy can provide very detailed structural information about growing chains (*via* the recognition of the effects on spectrum parameters of restricted rotation and chirality: see *e.g.* refs. 4 and 5); the second was to obtain kinetic parameters for the individual stages of the reaction, thus developing a steady-state approach recently utilized to determine the rate constants for addition of a variety of substituted alkyl radicals to acrylic acid and some related compounds.[6]

Results and Discussion

EPR experiments were carried out using a continuous-flow system to generate the initiating radical within the cavity of the spectrometer. Three solutions were mixed 30 ms before passage through the aqueous sample cell: the first contained Ti^{III}, to bring about decomposition of the peroxide (H_2O_2, $HO_2SO_3^-$, $P_2O_8^{4-}$), which was included in the second stream; and the third stream contained the appropriate monomer whose concentration was normally increased in successive experiments (see later). Experiments were normally carried out either at a final pH of *ca.* 2, achieved *via* the addition of sulfuric acid to stream (i), or a final pH of *ca.* 9, in which case the first stream contained the sodium salt of ethylenediaminetetraacetic acid (EDTA; and an appropriate quantity of ammonia). The initiating reactions which give rise to $^{\bullet}OH$, $SO_4^{-\bullet}$ and $PO_4^{2-\bullet}$ ($HPO_4^{-\bullet}$ at low pH) are described in reactions (1)–(3), respectively, and experiments involving $Cl_2^{-\bullet}$ were achieved by the addition of an excess of Cl^- to the $SO_4^{-\bullet}$-generating system [reactions (4) and (5)]; see ref. 7 and references therein. In the presence of a monomer (M) it is believed that addition of the initiating radical (*e.g.* $^{\bullet}OH$) will be followed by subsequent oligomerization for which the appropriate radicals may be detected [*e.g.* reactions (1) and (6)–(8)]. Computer-based analysis of steady-state concentrations detected in this way was achieved with an approach described previously.[6,7]

$$Ti^{III} + H_2O_2 \longrightarrow Ti^{IV} + {}^{\bullet}OH + OH^- \quad (1)$$

$$Ti^{III} + HO_2SO_3^- \longrightarrow Ti^{IV} + SO_4^{-\bullet} + OH^- \quad (2)$$

$$Ti^{III} + P_2O_8^{4-} \longrightarrow Ti^{IV} + PO_4^{2-\bullet} + PO_4^{3-} \quad (3)$$

$$SO_4^{-\bullet} + Cl^- \longrightarrow SO_4^{2-} + Cl^{\bullet} \quad (4)$$

$$Cl^{\bullet} + Cl^- \rightleftharpoons Cl_2^{-\bullet} \quad (5)$$

$$HO^{\bullet} + M \longrightarrow HO\text{-}M^{\bullet} \quad (M^{\bullet}) \quad (6)$$

$$HO\text{-}M^{\bullet} + M \longrightarrow HO\text{-}M\text{-}M^{\bullet} \quad (D^{\bullet}) \quad (7)$$

$$HO\text{-}M\text{-}M^{\bullet} + M \longrightarrow HO\text{-}M\text{-}M\text{-}M^{\bullet} \quad (T^{\bullet}) \quad (8)$$

Radical-initiated Reactions of Acrylic Acid.—*(i) EPR experiments.* The Ti^{III}–H_2O_2–acrylic acid [AA] system was first explored in experiments at pH *ca.* 2 in which the concentration of the monomer was increased (concentrations given in the legend to Fig. 1 and subsequently in this paper are those after mixing). The spectra at low acrylic acid concentration (see Fig. 1) clearly reveal both $^{\bullet}OH$ adducts, $HOCH_2\dot{C}HCO_2H$ (the β-adduct) and $^{\bullet}CH_2CH(OH)CO_2H$, (the α-adduct) (see Table 1); as [AA] is increased the concentration of the latter radical is reduced more quickly than the former, evidently because its rate of addition to the monomer is higher (as might be expected, since it is unsubstituted and non-conjugated). Extrapolation of these results to very low monomer concentrations gives a regioselectivity of $^{\bullet}OH$ attack (α:β) as 1:1.75.

Spectra recorded at higher monomer concentrations (*ca.* 10^{-2} mol dm^{-3}) reveal the presence of a dimer radical (▲) with non-equivalent β-protons—a signal probably augmented by overlap from the appropriate trimer (see below), for each of which chirality would render the β-CH_2 protons inequivalent.[5] The spectra also show traces of an extra radical (indicated ○) at high alkene concentrations ($\geqslant 5 \times 10^{-2}$ mol dm^{-3}): on the basis of the g value and the splitting [a(2H) 2.75 mT, which is

Table 1 EPR parameters of radicals produced in the reactions of acrylic and methacrylic acids at pH 2 and 9

Reaction	Radical formed	Hyperfine splitting/mT[a] a(α-H)	a(β-H)	a(γ-H)	g value[b]
CH_2=$CHCO_2H$/$^{\bullet}OH$	$^{\bullet}CH_2CH(OH)CO_2H$	2.21	2.68		2.002 50
	$HOCH_2\dot{C}HCO_2H$	2.04	2.73		2.003 10
	$HOCH_2CH(CO_2H)CH_2\dot{C}HCO_2H$	2.01	2.16(1), 2.27(1)		2.003 25
	~CH_2-$\dot{C}(CO_2H)$-CH_2~		*ca.* 2.75(2)		2.003 25
CH_2=$CHCO_2^-$/$^{\bullet}OH$	$^{\bullet}CH_2CH(OH)CO_2^-$	2.20	2.75		2.002 60
	$HOCH_2\dot{C}HCO_2^-$	2.04	2.75		2.003 15
	$HOCH_2CH(CO_2^-)CH_2\dot{C}HCO_2^-$	2.03	2.23(1), 2.56(1)	0.08	2.003 15
	$HO[CH_2CH(CO_2^-)]_2CH_2\dot{C}HCO_2^-$	2.08	2.50(1), 2.65(1)	0.09	2.003 15
	~CH_2-$\dot{C}(CO_2^-)$-CH_2~		2.73(2), 0.13(2)		2.003 25
CH_2=$CHCO_2H$/$SO_4^{-\bullet}$	$^-O_3SOCH_2\dot{C}HCO_2H$	2.07	2.53		*c*
	$^-O_3SOCH_2CH(CO_2H)CH_2\dot{C}HCO_2H$	2.04	2.17(1), 2.30(1)		*c*
CH_2=$CHCO_2^-$/$SO_4^{-\bullet}$	$^{\bullet}CH_2$-$CH(OSO_3^-)CO_2^-$	2.21	2.42		2.002 55
	$^-O_3SOCH_2\dot{C}HCO_2^-$	2.08	2.51		2.003 15
	$^-O_3SOCH_2CH(CO_2^-)CH_2\dot{C}HCO_2^-$	2.01	2.35(1), 2.61(1)	0.06	2.003 00
	$^-O_3SO[CH_2CH(CO_2^-)]_2CH_2\dot{C}HCO_2^-$	2.01	2.50(1), 2.65(1), 2.73(2)	0.09	2.003 00
	~CH_2-$\dot{C}(CO_2^-)$-CH_2~		0.13(2)		2.003 25
CH_2=$CMeCO_2H$/$^{\bullet}OH$	$^{\bullet}CH_2CMe(OH)CO_2H$	2.24		0.10 (Me)	2.002 50
	$HOCH_2\dot{C}MeCO_2H$[d]		1.96(2), 2.30(3)	0.11 (CO_2H)	2.003 05
			2.04(2), 2.30(3)	0.11 (CO_2H)	2.003 05
	$HOCH_2CMe(CO_2H)CH_2\dot{C}MeCO_2H$	2.24	2.39 (1 + 1)	0.10 (CO_2H)	2.003 20
CH_2=$CMeCO_2^-$/$^{\bullet}OH$	$HOCH_2\dot{C}MeCO_2^-$		2.27(3), 2.01(2)		2.003 20
	$HOCH_2CMe(CO_2^-)CH_2\dot{C}MeCO_2^-$		2.24(3), 1.72(1), 0.72(1)		2.003 05
	$HO[CH_2CMe(CO_2^-)]_2CH_2\dot{C}MeCO_2^-$		2.23(3), 1.79(1), 0.73(1)		2.003 05
CH_2=$CMeCO_2H$/$SO_4^{-\bullet}$	$^-O_3SOCH_2\dot{C}MeCO_2H$[d]		2.33(3), 1.85(2)	0.09 (CO_2H)	2.003 05
			2.33(3), 1.76(2)	0.09 (CO_2H)	2.003 05
	$^-O_3SOCH_2CMe(CO_2H)CH_2\dot{C}MeCO_2H$		2.27(3), 1.09(2)		2.003 20
	$^-O_3SO[CH_2CMe(CO_2H)]_2CH_2\dot{C}MeCO_2H$		2.27(3), 1.31(1), 0.87(1)		2.003 20
CH_2=$CMeCO_2^-$/$SO_4^{-\bullet}$	$^-O_3SOCH_2\dot{C}MeCO_2^-$		2.34(3), 1.77(2)		2.003 05
	$^-O_3SOCH_2CMe(CO_2^-)CH_2\dot{C}MeCO_2^-$		2.23(2), 2.66 (1 + 1)		2.003 05
	$^-O_3SO[CH_2CMe(CO_2^-)]_2CH_2\dot{C}MeCO_2^-$		2.23(3), 1.80(1), 0.70(1)		2.003 05

[a] ±0.005. [b] ±0.000 05. [c] Not measured. [d] Two rotamers.

Fig. 1 EPR spectra of the radicals produced during the hydroxyl-initiated polymerization of acrylic acid at pH *ca.* 2, showing the variation in the concentration of $^{\bullet}CH_2CH(OH)CO_2H$ (△), $^{\bullet}CH(CO_2H)CH_2OH$ (●), dimer (and trimer) (▲) and mid-chain (○) radicals with concentration of acrylic acid; $[Ti^{III}] = 1.67 \times 10^{-3}$ mol dm^{-3}, $[H_2O_2] = 1.67 \times 10^{-2}$ mol dm^{-3}; [AA] 4 × 10^{-3} (*a*), 1.5 × 10^{-2} (*b*), 4.8 × 10^{-2} mol dm^{-3} (*c*)

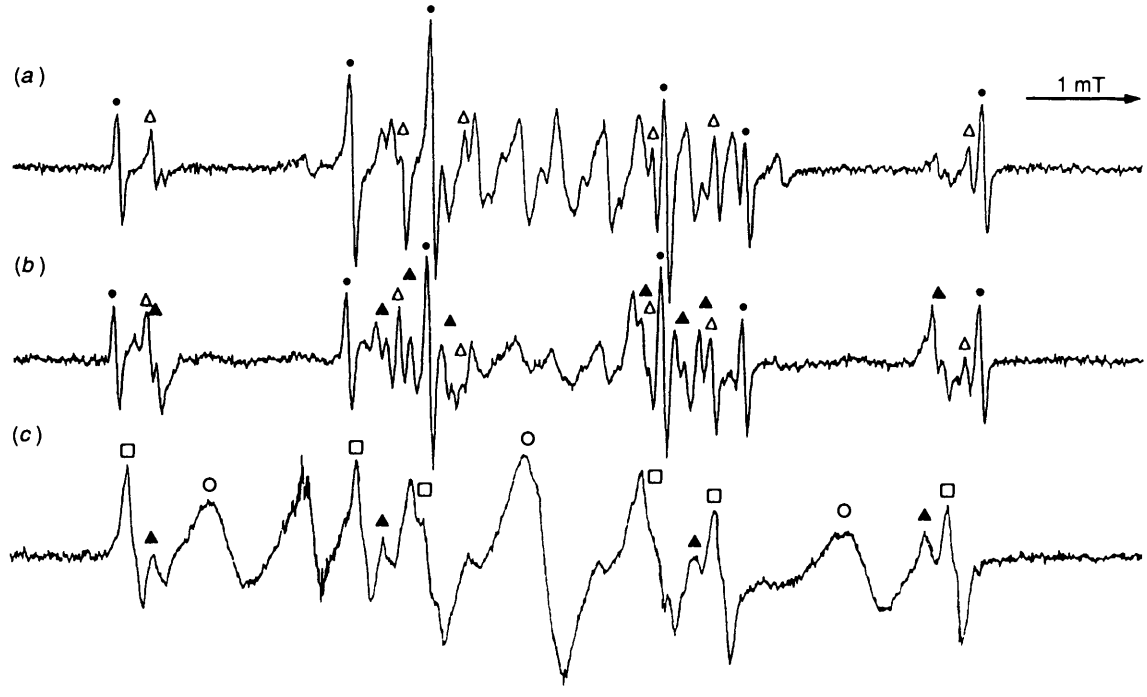

Fig. 2 EPR spectra of the radicals produced during the hydroxyl-initiated polymerization of acrylate anion at pH *ca.* 9, showing the variation in the concentration of $^{\bullet}CH_2CH(OH)CO_2^-$ (△), $^{\bullet}CH(CO_2^-)CH_2OH$ (●), dimer (▲), trimer (□) and mid-chain (○) radicals with concentration of acrylate anion; $[Ti^{III}$–EDTA] = 1.67 × 10^{-3} mol dm^{-3}, $[H_2O_2] = 1.67 \times 10^{-2}$ mol dm^{-3}; [AA] = 2.5 × 10^{-3} (*a*), 1.5 × 10^{-2} (*b*), 7.5 × 10^{-2} mol dm^{-3} (*c*)

attributed to β-protons] we propose that this is from a carboxyl-conjugated 'mid-chain' radical with structure $-CH_2-\dot{C}(CO_2H)-CH_2-$; further evidence for this assignment is given below.

Analogous experiments at p*H* 9 gave sharper-lined spectra which allowed the recognition of both $^{\bullet}OH$ adducts (regioselectivity 1:1.2, α:β) as well as distinct dimer, and trimer (head-to-tail) and mid-chain radicals (see Fig. 2 and Table 1). The dimer and trimer radicals both have non-equivalent β-proton splittings (as expected as a result of the adjacent asymmetric γ-carbon atom) and the prominent mid-chain radical shows evidence of further splitting. The variation in relative concentrations of the radicals detected at pH 2 and 9 as a function of monomer concentration is shown in Fig. 3.

Similar experiments were carried out with the sulfate radical-anion ($SO_4^{-\bullet}$) as the initiating agent: a typical example (at pH 9) is shown in Fig. 4. The line widths were usually sharp, enabling monomer (solely $^-O_3SOCH_2\dot{C}HCO_2H$ and its dianion), dimer and trimer radicals to be detected, and the extra splitting on the appropriate mid-chain radical is also revealed clearly. Traces of the β-OH adduct were also seen at low monomer concentration (see later).

The reaction of the chlorine radical-anion $Cl_2^{-\bullet}$ with acrylic acid gave the β-adduct $ClCH_2\dot{C}HCO_2H$ (for which the β-proton splittings suggest a bridged structure: see Table 2), together with a signal assigned to the appropriate dimer [*a*(α-H) 2.21, *a*(β-H) 2.03 mT]. In contrast to the reaction of $^{\bullet}OH$, no α-adduct was detected. We suggest that the lack of an observable α-adduct may be as a result of a rapid 1,2-shift in this isomer [see reaction (9)] which would be facilitated by chlorine-bridging and

associated stabilisation of the β-adduct. That such a rearrangement can occur is confirmed by our observation of both $MeĊClCO_2H$ [a(β-H) 2.10 (3 H), a(α-Cl) 0.27 mT, g 2.0056] and $ClCH_2ĊHCO_2H$ in the reaction between $HO^•$ and $MeCHClCO_2H$ under similar conditions: a lower limit for the rate constant for the 1,2 shift of Cl in $^•CH_2CHClCO_2H$ may therefore be estimated as 10^4 s^{-1}.[8]

$$^•CH_2CHClCO_2H \longrightarrow ClCH_2ĊHCO_2H \quad (9)$$

(*ii*) *Conformational and mechanistic conclusions.* The spectrum of the β-hydroxyl radical adduct of acrylic acid ($HOCH_2ĊHCO_2H$) shows an unusual line-width effect, the extreme lines being broader at low field than high field (see Fig. 1). This effect is unlikely to arise from rapid exchange of the acidic proton (in which case all lines would be broadened) but may reflect the occurrence of two closely similar overlapping spectra with very slightly different g- and a(β-H)-values. We associate this phenomenon, which was not observed above pH *ca.* 4, with the occurrence of restricted rotation about the Ċ–C(O) bond in the acid form, so that two isomers **1** and **2** are detected (an observation more clearly characterized for methacrylic acid — see later).

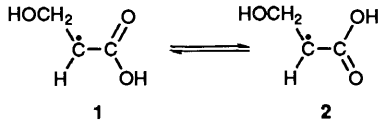

1 **2**

The non-equivalence observed in the β-proton splitting patterns of some dimers and trimers is believed to reflect the effect of an asymmetric carbon atom as neighbour,[5] though for the bigger and bulkier adducts (*e.g.* of $SO_4^{-•}$ and for the dimers and trimers) restricted rotation may also contribute [in which case significant differences in a(β-H) and broadening of the central lines of the 1:1:1:1 pattern might have been expected]. Conformational preferences are not particularly pronounced, as judged at least by the observation that most β-splittings are in the region of *ca.* 2.5 mT: for a radical of the type $RĊHCO_2H$, the parameter B [which largely governs the magnitude of a(β-H) through the $\rho B\cos^2\theta$ relationship], may be calculated as 4.6 mT, with a splitting of 2.3 mT calculated for the freely rotating CH_3 group.

To confirm the identity of the 'mid-chain' radical described earlier, we also studied the reactions of $^•OH$ with two samples of polyacrylic acid (Aldrich, average M_r 2000 and 90 000) at pH 2

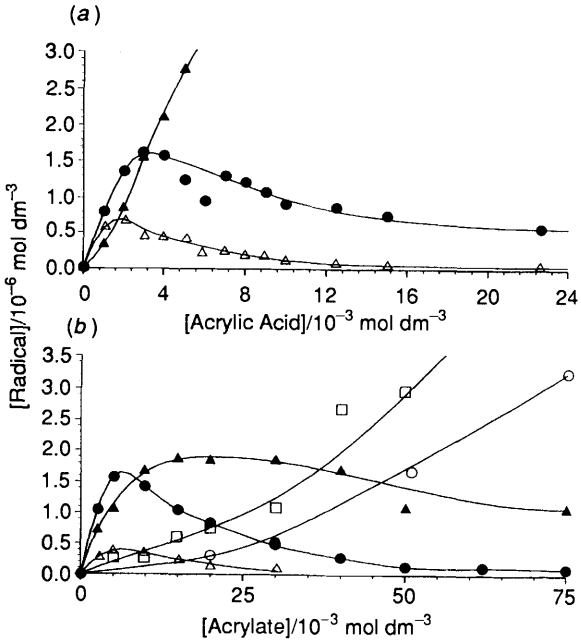

Fig. 3 (*a*) Variation in the concentration of $^•CH_2CH(OH)CO_2H$ (△), $^•CH(CO_2H)CH_2OH$ (●), and dimer radicals (▲) as a function of monomer concentration produced in the polymerization of acrylic acid initiated by Ti^{III} and H_2O_2 at pH *ca.* 2; $[Ti^{III}] = 1.67 \times 10^{-3}$ mol dm^{-3}, $[H_2O_2] = 1.67 \times 10^{-2}$ mol dm^{-3}. (*b*) Variation in the concentration of $^•CH_2CH(OH)CO_2^-$ (△), $^•CH(CO_2^-)CH_2OH$ (●), dimer (▲), trimer (□) and mid-chain (○) radicals as a function of alkene concentration produced in the polymerization of acrylate anion initiated by Ti^{III} and H_2O_2 at pH *ca.* 9; [Ti^{III}–EDTA] = 1.67×10^{-3} mol dm^{-3}, $[H_2O_2] = 1.67 \times 10^{-2}$ mol dm^{-3}.

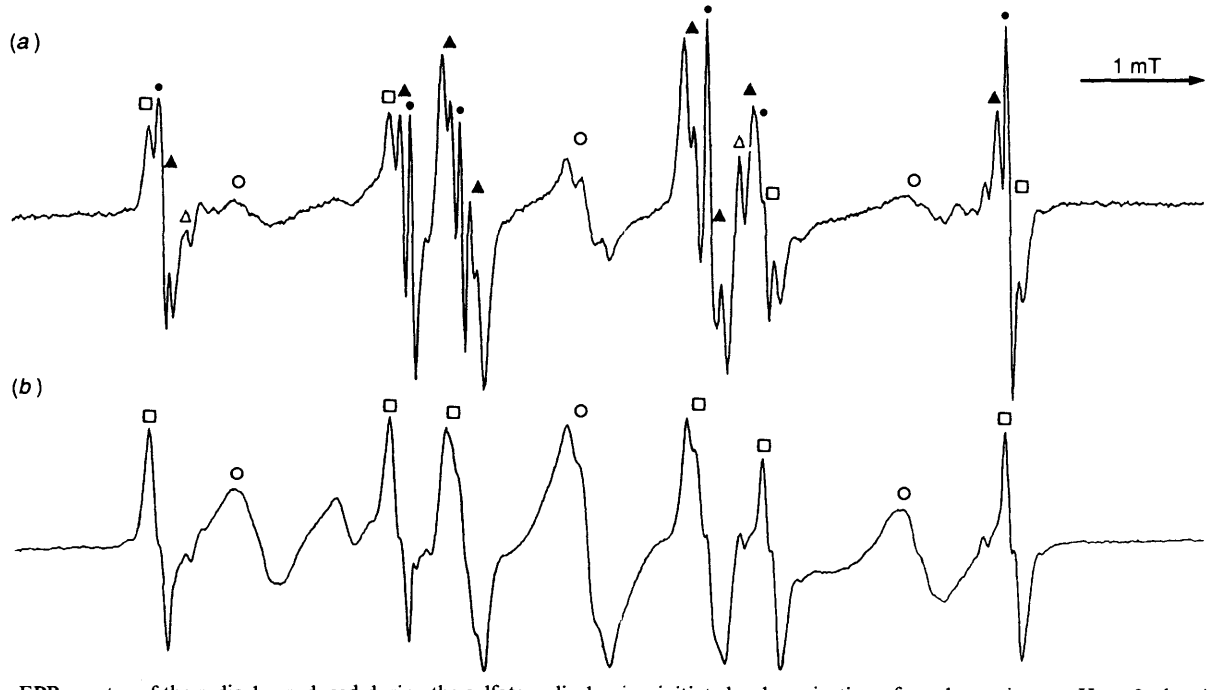

Fig. 4 EPR spectra of the radicals produced during the sulfate-radical-anion-initiated polymerization of acrylate anion at pH *ca.* 9, showing the variation in the concentration of $^•CH_2CH(OSO_3^-)CO_2^-$ (△), $^•CH(CO_2^-)CH_2OSO_3^-$ (●), dimer (▲), trimer (□) and mid-chain (○) radicals with concentration of acrylate anion; [Ti^{III}–EDTA] = 1.67×10^{-3} mol dm^{-3}, $[HO_2SO_3^-] = 1.0 \times 10^{-2}$ mol dm^{-3}; [AA] = 2.4×10^{-2} (*a*), 1.2×10^{-1} mol dm^{-3} (*b*)

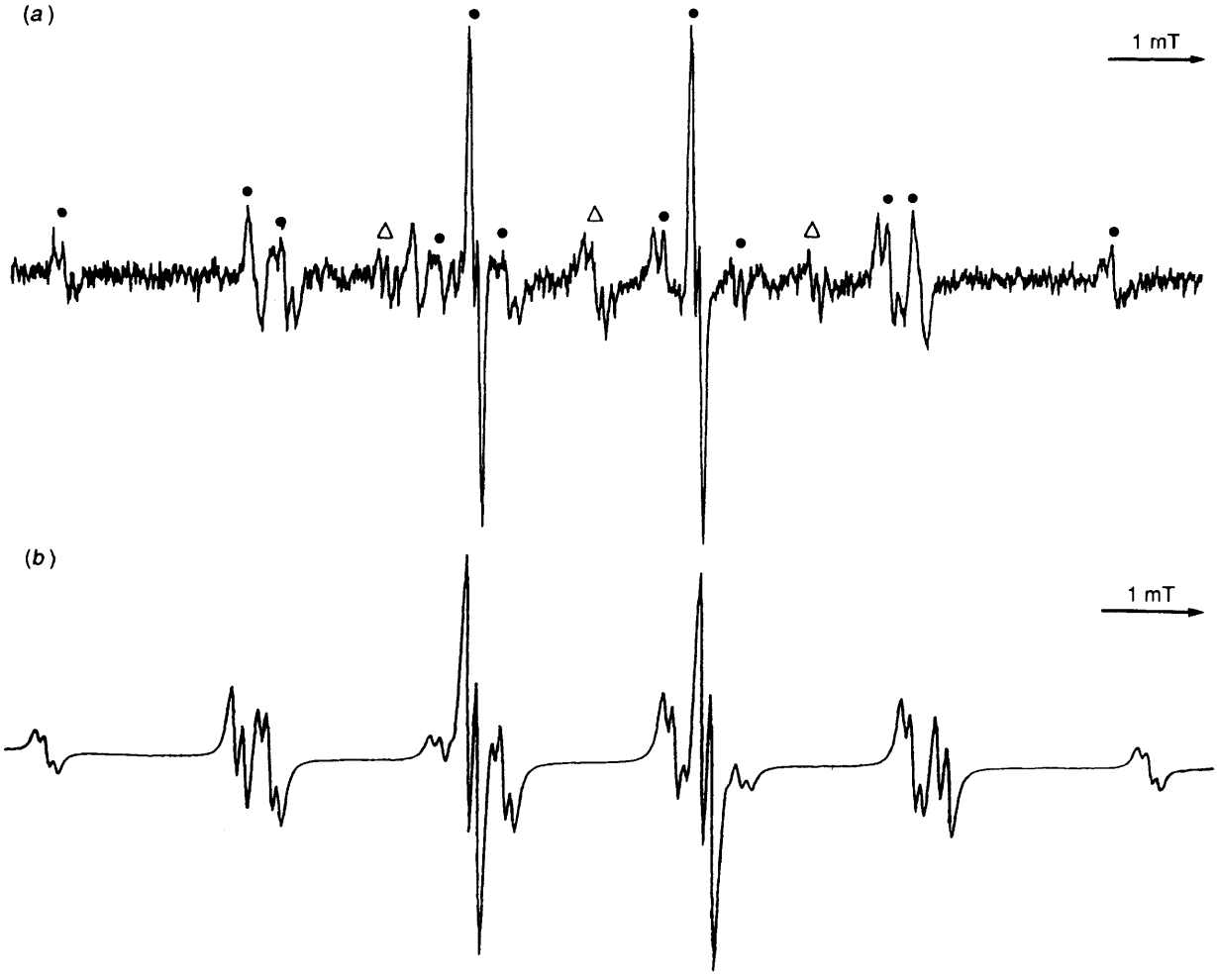

Fig. 5 (*a*) EPR spectrum of $^{\bullet}CMe(CO_2H)CH_2OH$ (●) produced in the polymerization of methacrylic acid at pH *ca.* 2, with low concentrations of $^{\bullet}CH_2CMe(OH)CO_2H$ (△); $[Ti^{III}] = 1.67 \times 10^{-3}$ mol dm^{-3}, $[H_2O_2] = 1.67 \times 10^{-2}$ mol dm^{-3}, [MA] = 2.5×10^{-3} mol dm^{-3}. (*b*) Simulated EPR spectrum of the two isomers of $^{\bullet}CMe(CO_2H)CH_2OH$ with (*i*) *a*(β-3H) 2.30, *a*(β-2H) 2.04 and *a*(CO_2H) 0.11 mT and (*ii*) *a*(β-3H) 2.30, *a*(β-2H) 1.96 and *a*(CO_2H) 0.11 mT.

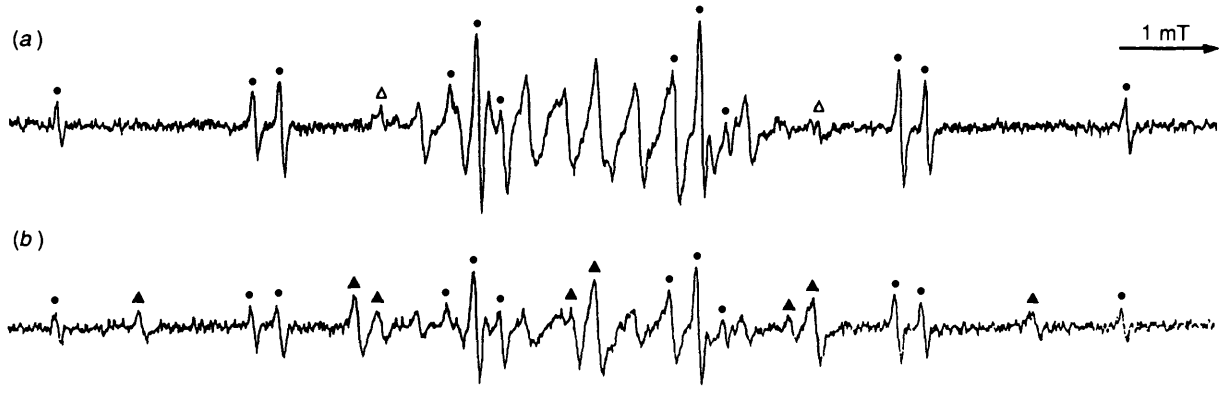

Fig. 6 EPR spectra of the radicals produced during the hydroxyl-initiated polymerization of methacrylate anion at pH *ca.* 9, showing the variation in the concentration of $^{\bullet}CH_2CMe(OH)CO_2^-$ (△), $^{\bullet}CMe(CO_2^-)CH_2OH$ (●) and dimer (▲) radicals with concentration of methacrylate anion; $[Ti^{III}$–EDTA$] = 1.67 \times 10^{-3}$ mol dm^{-3}, $[H_2O_2] = 1.67 \times 10^{-2}$ mol dm^{-3}; [MA] = 2.5×10^{-3} (*a*), 2.5×10^{-2} mol dm^{-3} (*b*)

and 9. In both cases, the spectra were dominated by a triplet with *a*(β-H) 2.74 mT (*i.e.* as observed in the polymerization of acrylic acid): in addition at pH 9 a further triplet (0.091 mT) was detected, exactly as described above. These radicals are assigned the structure **3** (and its ionized counterpart) with restriction of rotation about C_α–C_β: use of the equation for the angular dependence of β protons ($\rho B \cos^2 \theta$) leads to the conclusion that the appropriate dihedral angles (θ) for the β-protons are *ca.* 40 and 80°, as expected for a conformation (see *e.g.* **4**) in which the β–γ C–C bonds more or less eclipse the orbital of the unpaired electron. Similar spectra and conclusions have been reached on the basis of EPR spectra obtained during the photolysis of poly(hexane-1,6-diol) diacrylate.[9]

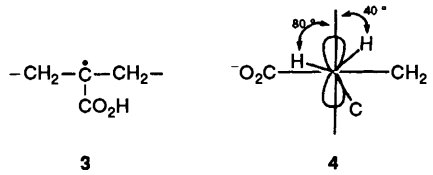

3 **4**

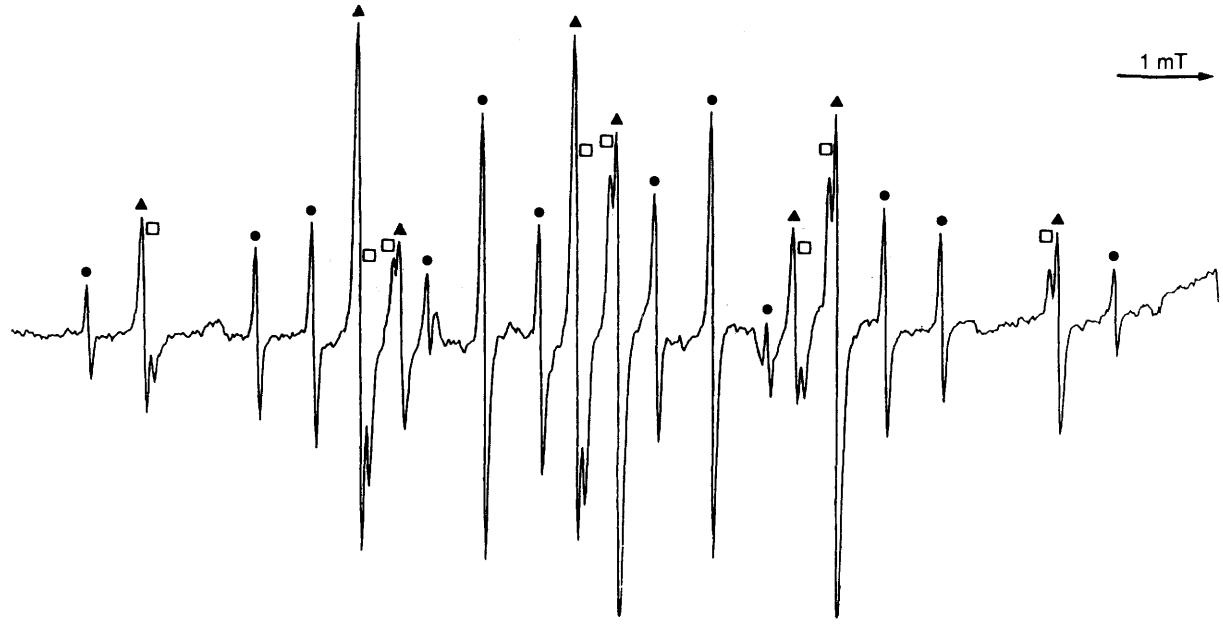

Fig. 7 EPR spectra of the radicals $^{\bullet}CMe(CO_2^-)CH_2OSO_3^-$ (●), dimer (▲) and trimer (□) produced during the sulfate-radical-anion-initiated polymerization of methacrylate anion at pH *ca.* 9; $[Ti^{III}\text{–EDTA}] = 1.67 \times 10^{-3}$ mol dm^{-3}, $[HOOSO_3^-] = 1.0 \times 10^{-2}$ mol dm^{-3}, [MA] = 10^{-1} mol dm^{-3}

Since radicals of type **3** are detected in the polymerization of acrylic acid only after the observation of monomer, dimer and trimer species as [AA] is increased, it can be concluded that they arise from the tetramer (and presumably higher oligomers) *via* 1,5-hydrogen shift, in a reaction which leads to the formation of a secondary, stabilized radical, and which obviously lowers the steady-state concentration of tetramer so that this is not detected (see Scheme 1).

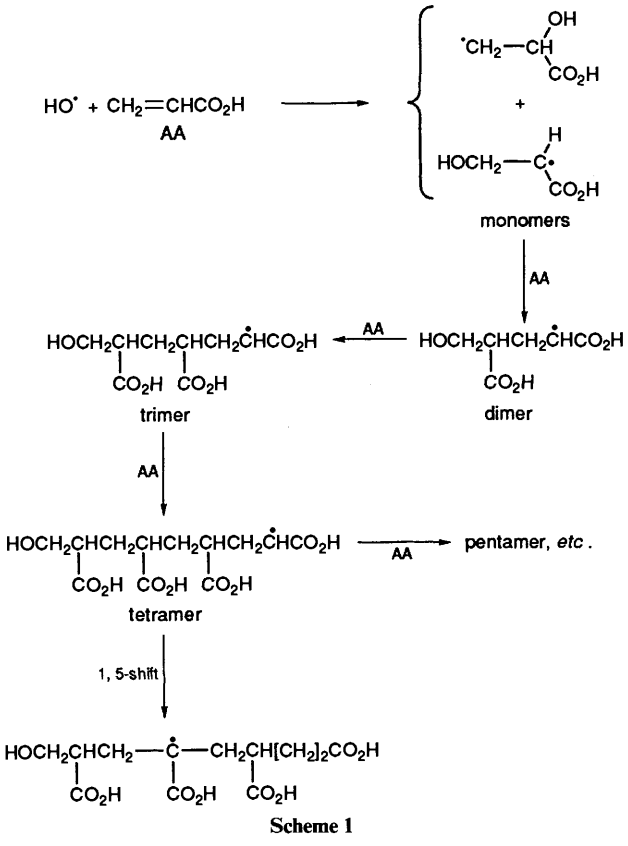

Scheme 1

Radical-initiated Reactions of Methacrylic Acid.—Related experiments with methacrylic acid confirm that •OH reacts

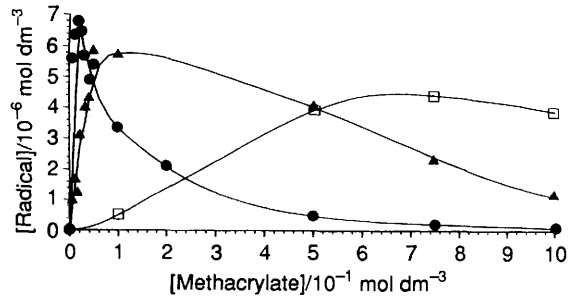

Fig. 8 Variation in the concentration of $^{\bullet}CMe(CO_2^-)CH_2OSO_3^-$ (●), dimer radicals (▲), trimer (□) as a function of monomer concentration produced in the polymerization of methacrylate anion initiated by Ti^{III} and $HOOSO_3^-$ at pH *ca.* 9; $[Ti^{III}\text{–EDTA}] = 1.67 \times 10^{-3}$ mol dm^{-3}, $[HOOSO_3^-] = 1.0 \times 10^{-2}$ mol dm^{-3}

largely at the unsubstituted end of the double bond (β) to give the monomer radical $HOCH_2\dot{C}MeCO_2H$ and then the head-to-tail dimer $HOCH_2CMe(CO_2H)CH_2\dot{C}MeCO_2H$ (at pH 2 and 9) and, at high pH, to give trimer (see Figs. 5 and 6, and Table 1); Fischer has reported similar behaviour for the methyl-radical-initiated polymerization. As shown in Fig. 5(*a*) [with its simulation in Fig. 5(*b*)] the radical $HOCH_2\dot{C}MeCO_2H$ exists in two isomeric forms, evidently as a result of restricted rotation about the C–C(O) bond as noted above (*cf.* with an expected stabilization energy for this type of radical of *ca.* 40 kJ mol^{-1}).[10]

In related experiments with the sulfate radical-anion, monomer, dimer and trimer radicals were detected at both low and high pH (see *e.g.* Fig. 7 and Table 1): line broadening in the middle line of the 1:1:1:1 β-proton pattern is very pronounced for the trimer (which, like the dimer, has non-equivalent β-proton splittings). The variation in steady-state concentrations of radicals with [methacrylic acid] in experiments at high pH is shown in Fig. 8.

The lower values of a(β-H) for methacrylate adducts (especially of $SO_4^{-\bullet}$ and at high pH) than their acrylate counterparts are as expected if conformations are now favoured in which the β C–X bond approaches more nearly the position in which it eclipses the unpaired electron (giving higher values of $\langle\theta\rangle$ for the β-protons). This is evidently a result of steric

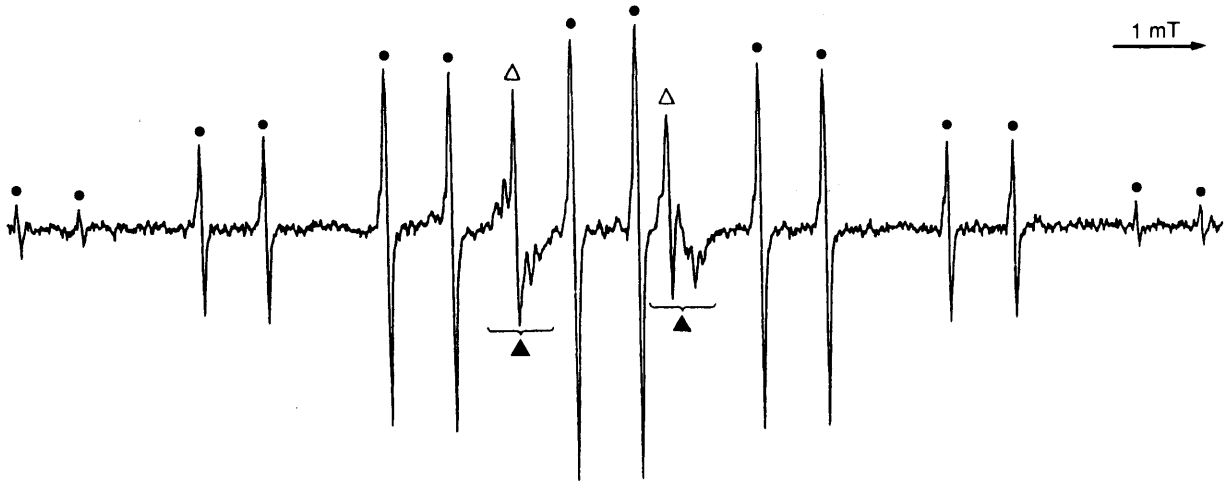

Fig. 9 EPR spectra of the radicals $^{\bullet}CMe_2CH(OSO_3^-)CO_2H$ (●), $^{\bullet}CH(CO_2H)CMe_2OSO_3^-$ (△) and $^{\bullet}CH(CO_2H)CMe_2OH$ (▲) produced by the addition of the sulfate-radical-anion to 3,3-dimethylacrylic acid at pH *ca.* 2; $[Ti^{III}] = 1.67 \times 10^{-3}$ mol dm^{-3}, $[HOOSO_3^-] = 1.0 \times 10^{-2}$ mol dm^{-3}, [3,3-DMA] = 7×10^{-3} mol dm^{-3}

hindrance involving the β substituent and the methyl and carboxy groups at the radical centre.

Reaction of $Cl_2^{-\bullet}$ with methacrylic acid gave signals from the β-adducts shown in Table 2.

EPR Studies of the Reactions of Initiating Radicals with Crotonic Acid and 3,3-Dimethylacrylic Acid.—The general reluctance of 1,2-substituted alkenes to undergo radical polymerization is illustrated by our results for the two alkenes crotonic and 3,3-dimethylacrylic acid under conditions similar to those employed for acrylic and methacrylic acids.

For example, $^{\bullet}OH$ adds on to both ends of the double bond for each alkene (see Table 3). The regioselectivity was found to depend upon the alkene and the pH (for the former the β : α ratio was 1 : 2.7 at pH 2, 1 : 2.4 at pH 9; for the latter, 1 : *ca.* 10 at pH 2, 1 : 1.1 at pH 9). No dimeric or trimeric radicals could be detected (even with [alkene] = 10^{-1} mol dm^{-3}), presumably because of the steric retardation from the β-methyl substituent(s); the regioselectivity of the reaction of $HO^{\bullet}$ with $Me_2C{=}CHCO_2H$ is notable.

Reaction of $SO_4^{-\bullet}$ with crotonic acid at pH 2 and 9 gave both α- and β-adducts (ratio *ca.* 2 : 1). With 3,3-dimethylacrylic acid the α- and β-adducts were accompanied by the β-hydroxyl adduct at pH 2 (see Table 3 and Fig. 9: very careful measurement was needed to distinguish the α-$SO_4^{-\bullet}$ adduct from the corresponding α-OH adduct). The effect of pH in the latter system was examined in more detail: as the pH was lowered from 2 to 1, the α-sulfate adduct was still observed but the β-sulfate adduct disappeared, being replaced by the β-OH adduct. At high pH, the α-$SO_4^{-\bullet}$ adduct was accompanied by the β-OH adduct, rather than the corresponding sulfate-substituted radical. We conclude that acid- and base-catalysed mechanisms must exist for converting the β-$SO_4^{-\bullet}$ adduct into the corresponding hydroxyl adduct (a type of reaction previously reported for certain electron-rich alkenes).[11] Possible acid- and base-catalysed mechanisms, related to the well-known S_N1 and S_N2 reactions respectively, are shown in Scheme 2.

With this substrate experiments were also conducted with $HPO_4^{2-\bullet}$ at low pH (*cf.* ref. 7); the behaviour resembled that of $SO_4^{-\bullet}$ under acidic conditions. At pH 2 the dominant signal was that of the β-adduct $^{\bullet}CH(CO_2H)CMe_2OPO_3H^-$, with *a*(1H) 1.90, *a*(P) 0.22 mT, *g* 2.0039, together with signal from $^{\bullet}CMe_2CH(OPO_3H^-)CO_2H$ and traces of the β-hydroxyl adduct [$^{\bullet}CH(CO_2H)CMe_2OH$: see Table 1]. As the pH was lowered, this signal grew in intensity at the expense of the β-phosphate precursor [*cf.* reaction of $SO_4^{-\bullet}$ adducts].

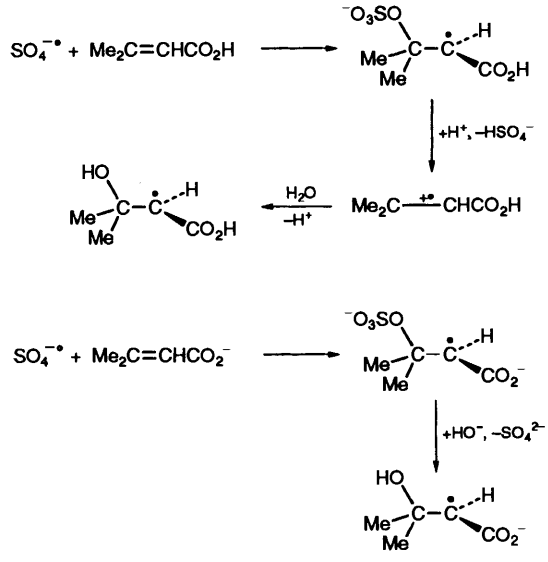

Scheme 2

With $Cl_2^{-\bullet}$ at pH 2, signals were detected from the β-chlorine adducts $^{\bullet}CH(CO_2H)CHMeCl$ and $^{\bullet}CH(CO_2H)CMe_2Cl$ (see Table 2) from crotonic acid and 3,3-dimethylacrylic acids, respectively; for the latter, weak signals (which increased at high pH) were also observed from the corresponding α- and β-hydroxyl adducts. This suggests that, at least for the latter substrate, chlorine addition at both carbon atoms is followed by hydrolysis (also subject to base catalysis) of the C–Cl bond, as noted above for sulfate adducts. At low pH this may well reflect the loss of chloride ion and give a radical-cation, encouraged by the electron-donating effect of the methyl substituents.

Kinetic Analysis via *the Analysis of Steady-state Concentrations.*—Kinetic simulations were next carried out in an attempt to determine rate constants for both propagation and radical–radical termination reactions; we have fitted the variation in observed radical concentration with the concentration of alkene in a computer-based approach described previously. We have based our analysis on the reactions shown in Scheme 3 (*e.g.* for acrylic acid) with $k_1 = 2.1 \times 10^3$ dm^3 mol^{-1} s^{-1}.[12] A number of other assumptions have been made in the reaction model employed for polymerization; for example, we have assumed that polymerization is only terminated by radical–radical reactions, rather than by reaction of organic radicals with H_2O_2, Ti^{III} or Ti^{IV} (we believe that this is justified for the

Table 2 EPR parameters for β-chlorine radicals formed by the addition of Cl$^{\bullet}$ to acrylic monomers

Reaction	Radical, R$^{\bullet}$	Hyperfine splitting/mT[a] a(α-H)	a(β-H)	a(Cl)	a(γ-H)	g value[b]
CH_2=$CHCO_2H$	$ClCH_2\dot{C}HCO_2H$	2.04	1.18	1.18		2.003 30
	$ClCH_2\dot{C}HCO_2^-$	2.03	1.09	1.40		2.003 30
CH_2=$CMeCO_2H$	$ClCH_2\dot{C}MeCO_2H$		2.26, 0.86	1.18		2.003 30
	$ClCH_2\dot{C}MeCO_2^-$		2.24, 0.82	1.42		2.003 30
MeCH=$CHCO_2H$	$ClCHMe\dot{C}HCO_2H$	2.06	0.76	1.20	0.05	2.003 20
	$ClCHMe\dot{C}HCO_2^-$	2.18	1.65	0.68	0.07	2.003 05
Me_2C=$CHCO_2H$	$ClCMe_2\dot{C}HCO_2H$	1.96	—	1.01	0.08	2.003 50

[a] ±0.01. [b] ±0.000 05.

Table 3 EPR parameters of the radicals produced by the addition of hydroxyl radicals and $SO_4^{-\bullet}$ to crotonic acid and 3,3-dimethylacrylic acid at pH 2 and pH 9

Reaction	Radical formed	Hyperfine splitting/mT[a] a(α-H)	a(β-H)	a(γ-H)	g value[b]
MeCH=$CHCO_2H$/$^{\bullet}OH$	$Me\dot{C}H$–$CH(OH)CO_2H$	2.19	1.62(1), 2.57(3)		2.002 45
	$MeCH(OH)$–$\dot{C}HCO_2H$	2.06	1.61	0.13	2.003 20
MeCH=$CHCO_2H$/$SO_4^{-\bullet}$	$Me\dot{C}H$–$CH(OSO_3^-)CO_2H$	2.20	1.44(1), 2.59(3)		2.002 60
	$MeCH(OSO_3^-)$–$\dot{C}HCO_2H$	2.06	1.20	0.18	2.003 15
MeCH=$CHCO_2^-$/$^{\bullet}OH$	$Me\dot{C}H$–$CH(OH)CO_2^-$	2.16	1.56(1), 2.55(3)		2.002 75
	$MeCH(OH)$–$\dot{C}HCO_2^-$	2.04	1.58	0.15	2.003 25
MeCH=$CHCO_2^-$/$^{\bullet}OH$	$Me\dot{C}H$–$CH(OSO_3^-)CO_2^-$	2.17	1.34(1), 2.57(3)		2.002 69
	$MeCH(OSO_3^-)\dot{C}HCO_2^-$	2.07	1.35	0.18	2.003 17
Me_2C=$CHCO_2H$/$^{\bullet}OH$	$Me_2\dot{C}$–$CH(OH)CO_2H$	—	0.84(1), 2.34(6)		2.002 70
	$Me_2C(OH)$–$\dot{C}HCO_2H$	2.07	—	0.12	2.003 15
$Me_2C^{=}CHCO_2H$/$SO_4^{-\bullet}$	$Me_2\dot{C}$–$CH(OSO_3^-)CO_2H$	—	0.81(1), 2.34(6)		2.002 75
	$Me_2C(OSO_3^-)\dot{C}HCO_2H$	1.92			2.003 65
Me_2C=$CHCO_2^-$/$^{\bullet}OH$	$Me_2\dot{C}$–$CH(OH)CO_2^-$	—	0.75(1), 2.32(6)		2.002 70
	$Me_2C(OH)$–$\dot{C}HCO_2^-$	2.06	—	0.13	2.003 10
Me_2C=$CHCO_2^-$/$SO_4^{-\bullet}$	$Me_2\dot{C}$–$CH(OSO_3^-)CO_2^-$	—	0.72(1), 2.33(6)		2.002 75
	$Me_2C(OH)$–$\dot{C}HCO_2^-$	2.06		0.13	2.003 05

carboxyl-conjugated radicals involved). On the other hand, at low alkene concentrations, the addition of the hydroxyl radical to the monomer is expected to be in competition with its reaction with Ti^{III} and H_2O_2 [reactions (15) and (16)] and these reactions have been included (with rate constants of 2×10^9 and 2.7×10^7 dm^3 mol^{-1} s^{-1}, respectively).[12] The rate of cross termination of two radicals of different self-termination rate constants was taken as the square root of the product of the two self-termination rate constants.

(*i*) *Reaction of* HO$^{\bullet}$ *with acrylic acid and related compounds at* pH 2.0. The simulated variation of the concentration of the α- and β-radical adducts of acrylic acid at relatively low monomer concentration was first estimated, using a reaction scheme which involved initiation to give HO$^{\bullet}$, reaction of HO$^{\bullet}$ with the monomer to give the α- and β-adducts as well as with Ti^{III} and H_2O_2, propagation of α- and β-adducts (to give dimer radicals, D$^{\bullet}$) and radical–radical termination reactions (see Scheme 3). The overall rate constant for addition of hydroxyl to acrylic acid was taken as 1.4×10^9 dm^3 mol^{-1} s^{-1},[12] and the different rate constants of addition at the two alkenic carbons determined for the proportion of each adduct seen at low monomer concentration. The rate constants for radical–radical termination reactions ($2k_t$) were initially taken to be 2×10^9 dm^3 mol^{-1} s^{-1} with a similar value for self-termination of the dimer.[13,14]

Reasonable agreement with the observed concentrations for

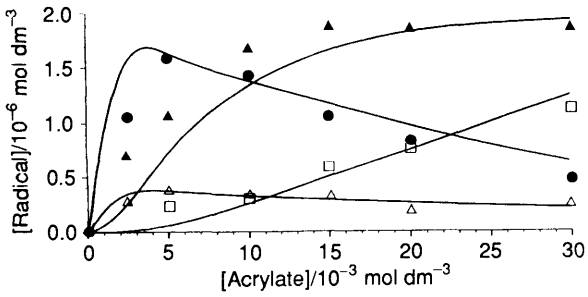

Fig. 10 Experimental and simulated variation of $^{\bullet}CH_2CH(OH)CO_2^-$ (△), $^{\bullet}CH(CO_2^-)CH_2OH$ (●), dimer (▲) and trimer (□) radical concentrations with monomer concentration in the hydroxyl-initiated polymerization of acrylate anion at pH *ca.* 9. The solid lines represent the simulated data. For the rate constants used for the simulation see the text.

α- and β-adducts was achieved when the rate constants of propagation were in the range 1–3 × 10^6 dm^3 mol^{-1} s^{-1} for the α-adduct [$^{\bullet}CH_2CH(OH)CO_2H$] and 2–6 × 10^5 dm^3 mol^{-1} s^{-1} for the β-adduct [$^{\bullet}CH(CO_2H)CH_2OH$]. Refinement of the rate constants gave optimal values for k_p of 3 × 10^6 and 4 × 10^5 dm^3 mol^{-1} s^{-1} for $^{\bullet}CH_2CH(OH)CO_2H$ (α) and $^{\bullet}CH(CO_2H)CH_2OH$ (β), respectively. As expected, the value of the former is somewhat greater than the latter which is retarded for both steric and electronic reasons. As would be expected, the rate constants for addition to acrylic acid of the α- and β-adducts are very similar to those obtained for the reaction of propanoic acid-derived radicals to the same alkene ($^{\bullet}CH_2CH_2CO_2H$, 3 × 10^6; $^{\bullet}CHMeCO_2H$, 3 × 10^5 dm^3 mol^{-1} s^{-1}).[6]

$$Ti^{III} + H_2O_2 \longrightarrow Ti^{IV} + HO^- + HO^{\bullet} \quad (1)$$

$$HO^{\bullet} + CH_2{=}CHCO_2H \longrightarrow {}^{\bullet}CH_2CH(OH)CO_2H \quad (R^{\bullet}_{\alpha}) \quad (10)$$

$$HO^{\bullet} + CH_2{=}CHCO_2H \longrightarrow {}^{\bullet}CH(CO_2H)CH_2OH \quad (R^{\bullet}_{\beta}) \quad (11)$$

$$R^{\bullet}_{\alpha} + CH_2{=}CHCO_2H \longrightarrow \text{Dimer } (D^{\bullet}) \quad (12)$$

$$R^{\bullet}_{\beta} + CH_2{=}CHCO_2H \longrightarrow \text{Dimer } (D^{\bullet}) \quad (13)$$

$$R^{\bullet} + R^{\bullet} \longrightarrow \text{Non-radical products} \quad (14)$$

$$HO^{\bullet} + Ti^{III} \longrightarrow HO^- + Ti^{IV} \quad (15)$$

$$HO^{\bullet} + H_2O_2 \longrightarrow H_2O + HO_2^{\bullet} \quad (16)$$

Scheme 3

A similar approach was employed for the simulation of the observed concentration of radicals from the reaction of methacrylic acid with hydroxyl at pH 2: addition of $HO^{\bullet}$ to methacrylic acid was assumed to occur solely at the β-position, to give $^{\bullet}CMe(CO_2H)CH_2OH$ with a rate constant of 2.9 × 10^9 dm^3 mol^{-1} s^{-1},[12] and the rate constant for all radical–radical termination reactions ($2k_t$) was taken as 10^9 dm^3 mol^{-1} s^{-1} [*cf.* $2k_t$ for $^{\bullet}CMe_2CO_2H$].[14] A reasonably good fit for the variation of the concentrations of both monomer and dimer radicals with alkene was then obtained using a propagation rate constant, k_p, of 3 × 10^5 dm^3 mol^{-1} s^{-1}.

(*ii*) *Reaction of* $HO^{\bullet}$ *with acrylate anion and related compounds at* pH 9.0. The hydroxyl-initiated polymerization of the acrylate anion was simulated using a scheme similar to that used for acrylic acid. The reaction of the hydroxyl radical with EDTA was included (2.6 × 10^9 dm^3 mol^{-1} s^{-1})[12] and the overall rate constant for $HO^{\bullet}$ addition was taken as 5.7 × 10^9 dm^3 mol^{-1} s^{-1}.[12]

The variation of monomer and dimer radicals at low monomer concentrations was initially simulated using $2k_t$ for all radical terminations as 2 × 10^9 dm^3 mol^{-1} s^{-1}. Although a reasonable fit was obtained for the variation of the two monomer radicals (with $k_{p\beta}$ 2 × 10^5 dm^3 mol^{-1} s^{-1} and $k_{p\alpha}$ 3 × 10^5 dm^3 mol^{-1} s^{-1}) the predicted concentration of the dimer radicals was lower than observed. This is believed to reflect the fact that the rate constants of termination of the radicals (in particular that for the dimer radicals) may be lower due to charge repulsion. Reduction of the rate constant for dimer–dimer reaction to 5 × 10^8 dm^3 mol^{-1} s^{-1} leads to a much better fit to the experimental data (see Fig. 10); $2k_t$ for $^{\bullet}CH(CO_2^-)CH_2OH$ was also reduced to 1.5 × 10^9 dm^3 mol^{-1} s^{-1}.

The simulation was then extended to higher monomer concentration where significant addition of the dimer radical to more alkene, to give trimer, is observed. A good fit between experimental and simulated radical concentrations was achieved by employing rate constants of 5 × 10^4 dm^3 mol^{-1} s^{-1} for the addition of the dimer radical to alkene, with 4 × 10^8 dm^3 mol^{-1} s^{-1} for the rate constant of the dimerisation of the trimer radicals (with triple negative charge). On the assumption that the rate constants for addition of the trimer radical to alkene is similar to that for the dimer, and dimerisation of the tetramer radical is similar to that for the trimer, it is possible to estimate that the rate constant for intramolecular hydrogen-abstraction is *ca.* 1 × 10^3 s^{-1}.

The reaction of $HO^{\bullet}$ with methacrylate anion was simulated in similar fashion. The rate of addition to methacrylate anion was taken as 1.6 × 10^{10} dm^3 mol^{-1} s^{-1}.[12] Reasonable agreement with experimental data was achieved when k_p was taken as 2 × 10^5 dm^3 mol^{-1} s^{-1} although it was surprising that the rate constants for dimer–dimer radical termination did not require lowering (as was the case for the acrylate anion) and as might be expected for the reaction of two di-negatively charged species.[13]

(*iii*) *Reaction of* $SO_4^{-\bullet}$ *with acrylate anion and related compounds at* pH 9.0. Simulation of the reaction of $SO_4^{-\bullet}$ with the acrylate anion at pH 9.0 was also attempted. A scheme analogous to that for addition of $HO^{\bullet}$ to acrylate was used. As explained earlier, initiation was brought about by the reaction of titanium(III) with peroxymonosulfate ($HO_2SO_3^-$) [with a rate constant of 1.3 × 10^3 dm^3 mol^{-1} s^{-1}, reaction (2)] with $SO_4^{-\bullet}$ addition to alkene in competition with reduction by titanium(III) [reaction (17)]. Reaction of HO^- with $SO_4^{-\bullet}$ [reaction (18)] was included in the scheme (since $HO^{\bullet}$ adducts to the alkene were observed) with a rate constant of 6.5 × 10^7 dm^3 mol^{-1} s^{-1}.[15] The rate constant for addition of $SO_4^{-\bullet}$ to acrylate anion[15] was taken as 1.1 × 10^8 dm^3 mol^{-1} s^{-1} and was adjusted to account for differences in the regioselectivity of addition.

$$HOOSO_3^- + Ti^{III} \longrightarrow HO^- + SO_4^{-\bullet} + Ti^{IV} \quad (2)$$

$$SO_4^{-\bullet} + Ti^{III} \longrightarrow SO_4^{2-} + Ti^{IV} \quad (17)$$

$$SO_4^{-\bullet} + HO^- \longrightarrow SO_4^{2-} + HO^{\bullet} \quad (18)$$

The rate constants for reaction of the α- and β-adducts with alkene and those for radical–radical reactions were optimised at low alkene concentration. This gave predicted rate constants, k_p, of 5 × 10^4 and 1 × 10^5 dm^3 mol^{-1} s^{-1} for $^{\bullet}CH(CO_2^-)CH_2OSO_3^-$ and $^{\bullet}CH_2CH(OSO_3^-)CO_2^-$, respectively. Radical termination rate constants were taken as 7 × 10^8 dm^3 mol^{-1} s^{-1} for monomer–monomer and 2.4 × 10^8 dm^3 mol^{-1} s^{-1} for dimer–dimer reactions. The subsequent addition of dimer radical to alkene was also modelled at higher alkene concentration. The rate constant for addition is estimated to be

Table 4 Rate constants for initial stages of radical-initiated alkene polymerisation reactions determined by kinetic simulations of steady-state concentrations

Initiator	Alkene	Rate constant[a]/dm^3 mol^{-1} s^{-1}					
		k_p (β-adduct + monomer)	k_p (α-adduct + monomer)	k_p (dimer radical + monomer)	$2k_t$ (β-adduct)	$2k_t$ (α-adduct)	$2k_t$ (dimer radical)
HO$^\bullet$	CH_2=$CHCO_2H$	4×10^5	3×10^6	—	2×10^9	2×10^9	2×10^9
HO$^\bullet$	CH_2=$CMeCO_2H$	3×10^5	—	—	1×10^9	—	1×10^9
HO$^\bullet$	CH_2=$CHCO_2^-$	2×10^5	3×10^5	5×10^4	1.5×10^9	2×10^9	5×10^8
HO$^\bullet$	CH_2=$CMeCO_2^-$	2×10^5	—	—	2×10^9	—	2×10^9
$SO_4^{-\bullet}$	CH_2=$CHCO_2^-$	5×10^4	1×10^5	1×10^4	7×10^8	7×10^8	2.4×10^8
$SO_4^{-\bullet}$	CH_2=$CMeCO_2^-$	2.5×10^4	—	$1–5 \times 10^3$	2×10^8	—	8×10^7

[a] ±10%.

ca. 1×10^4 dm^3 mol^{-1}, s^{-1}, although the variation in trimer concentration could not be satisfactorily modelled.

The variation of radical concentrations with methacrylate anion concentration for the $SO_4^{-\bullet}$-initiated polymerization was simulated using a scheme similar to that for $SO_4^{-\bullet}$ reaction with acrylate anion. As with the simulations of HO$^\bullet$ with methacrylate anion, only formation of the α-radical [$^\bullet$CMe-(CO_2^-)$CH_2OSO_3^-$] was considered in the mechanism. At low monomer concentration, reasonable agreement with experimental data could be obtained with k_p for $^\bullet$CMe(CO_2^-)-$CH_2OSO_3^-$ with methacrylate as 2.5×10^4 dm^3 mol^{-1} s^{-1} and $2k_t$ for monomer–monomer and dimer–dimer radical terminations as 2×10^8 and 8×10^7 dm^3 mol^{-1} s^{-1}, respectively. The behaviour at higher monomer concentrations could not be simulated satisfactorily (*i.e.* when trimer formation is significant) although it is believed that k_p for dimer radical addition to alkene is in the range $1–5 \times 10^3$ dm^3 mol^{-1} s^{-1}.

Conclusions

Our experiments illustrate how continuous-flow techniques and EPR spectroscopy can provide structural and kinetic information on the initial stage of metal-catalysed and free-radical-initiated alkene polymerization. Direct evidence for intramolecular hydrogen-abstraction in growing acrylate chains has also been obtained. The kinetic results provide estimates for the rate constants of initial stages of propagation (monomer to dimer, dimer to trimer) and termination reactions, the latter as a function of size (monomer, dimer, *etc.*) and overall charge (*i.e.* at high and low pH values). Propagation rate constants for the initial steps are found to be significantly greater than those reported for similar bulk polymerisation reactions [for example, k_p for $^\bullet$CH(CO_2H)CH_2OH addition to CH_2=$CHCO_2H$ is 4×10^5 dm^{-3} mol^{-1} s^{-1}, compared with *ca.* 10^3 dm^{-3} mol^{-1} s^{-1} for related acrylate and methacrylate polymerisations].[16] This is presumably due to differences in the rates of diffusion of the radical species (due to steric and viscosity changes) although solvent effects may also be significant.[17]

Experimental

EPR spectra were recorded on a Bruker ESP 300 spectrometer equipped with an X-band microwave bridge and 100 kHz modulation. Hyperfine splittings and *g* values were determined directly from the spectrometer's field scan, this having been calibrated with the signal from Fremy's salt (a_N = 1.3091 mT,[18] *g* 2.0055[19]). Radical concentrations were determined by comparison with spectra obtained from standard solutions of vanadyl sulfate by use of double integration. A mixing chamber was employed which allowed simultaneous mixing of three reagent streams *ca.* 30 ms before passage through the cavity of the spectrometer: flow was maintained using a Watson–Marlow 502S peristaltic pump placed on the inlet tubing. pH measurements were made using a Pye-Unicam PW9410 pH meter with the electrode inserted into the effluent stream. The three solutions typically contained (*i*) titanium(III) chloride (0.005 mol dm^{-3}), (*ii*) the peroxide (H_2O_2 0.05 mol dm^{-3} or $HOOSO_3^-$ 0.01 mol dm^{-3}) and (*iii*) the substrate (0.05 to 1.0 mol dm^{-3}) and the alkene (0.0005 to 0.01 mol dm^{-3}); pH was varied by addition of sulfuric acid (18 mol dm^{-3}) or ammonia solution (15 mol dm^{-3}) to the first stream and all solutions were deoxygenated by nitrogen purge both before and during use. EDTA (0.006 mol dm^{-3}) was added to the titanium(III) stream in experiments carried out at pH 9. Cl$^\bullet$ and $Cl_2^{\bullet-}$ were generated by the addition of sodium chloride (0.03–3.0 mol dm^{-3}) to the substrate stream.

The kinetic simulation program was originally written by Dr. T. M. F. Salmon and modified to run on a VAX computer (by Dr. M. J. Brown) and on an IBM-PC 486DX clone.

All chemicals employed were commercial samples used as supplied.

Acknowledgements

Support from the SERC and ICI Paints plc is gratefully acknowledged. We also thank Dr. E. C. Nield for helpful discussions.

References

1 H. Fischer, *Polym. Lett.*, 1964, **2**, 529.
2 H. Fischer, *Adv. Poly. Sci., Part C*, 1968, **5**, 463.
3 H. Fischer, *Makromol. Chem.*, 1966, **98**, 179.
4 J. K. Kochi, *Adv. Free-radical Chem.*, 1975, **5**, 189.
5 B. C. Gilbert and M. Trenwith, *J. Chem. Soc., Perkin Trans. 2*, 1973, 1834.
6 B. C. Gilbert, J. R. Lindsay Smith, E. C. Milne, A. C. Whitwood and P. Taylor, *J. Chem. Soc., Perkin Trans. 2*, 1993, 2025.
7 B. C. Gilbert, J. K. Stell, W. J. Peet and K. J. Radford, *J. Chem. Soc., Faraday Trans. 1*, 1988, **84**, 3319.
8 A. L. J. Beckwith and P. K. Tindal, *Aust. J. Chem.*, 1971, **24**, 2099.
9 M. E. Best and P. H. Kasai, *Macromolecules*, 1989, **22**, 2622.
10 W. Lung-Min and H. Fischer, *Helv. Chim. Acta*, 1983, **66**, 138.
11 M. J. Davies and B. C. Gilbert, *J. Chem. Soc., Perkin Trans. 2*, 1984, 1809.
12 (*a*) Farhataziz and A. B. Ross, *Selected Specific Rates of Reactions of Transients from H_2O in Aqueous Solution. III. Hydroxyl Radical and Perhydroxyl Radicals and their Radical Ions*, National Bureau of Standards, Washington, 1977; (*b*) G. V. Buxton, C. L. Greenstock, W. P. Helman and A. B. Ross, 'Critical Review of Rate Constants for Reactions of Hydrated Electrons, Hydrogen Atoms and Hydroxyl Radicals ($HO^\bullet/^\bullet O^-$) in Aqueous Solution', *J. Phys. Chem. Ref. Data*, 1988, **17**, 513.

13 P. Neta, *Adv. Phys. Org. Chem.*, 1976, **12**, 223.
14 P. Neta, M. Simic and E. Hayon, *J. Phys. Chem.*, 1969, **73**, 4207.
15 A. B. Ross and P. Neta, *Rate Constants for Reactions of Inorganic Radicals in Aqueous Solution*, National Bureau of Standards, Washington, 1979.
16 R. Sack, G. V. Schulz and G. Meyerhoff, *Macromolecules*, 1988, **21**, 3345.
17 V. F. Gromov, N. I. Galperina, T. O. Osmanov, P. M. Khomikovski and A. D. Abkin, *Eur. Polym. J.*, 1980, **16**, 529.
18 R. J. Faber and G. K. Fraenkel, *J. Chem. Phys.*, 1967, **47**, 2462.
19 J. Q. Adams, S. W. Nicksic and J. R. Thomas, *J. Chem. Phys.*, 1966, **45**, 654.

Paper 4/01774I
Received 24*th March* 1994
Accepted 3*rd May* 1994